PNAS Nexus, 2026, **5**, pgag176
https://doi.org/10.1093/pnasnexus/pgag176
Published: 31 May 2026
Research Report

Paradoxical coexistence of superconductivity and magnetism, and explaining unexpected preferred domain orientations

Shoham Sen[1], **Liping Liu**[2,3]*, **and Pradeep Sharma**[1,4,5]*

[1]Department of Materials Science and Engineering, University of Houston, 4226 Martin Luther King Boulevard, Houston, TX 77204, United States
[2]Department of Mathematics, Rutgers University, Piscataway, NJ 08854, United States
[3]Department of Mechanical and Aerospace Engineering, Rutgers University, Piscataway, NJ 08854, United States
[4]Department of Physics, University of Houston, 4226 Martin Luther King Boulevard, Houston, TX 77204, United States
[5]Department of Mechanical and Aerospace Engineering, University of Houston, 4226 Martin Luther King Boulevard, Houston, TX 77204, United States
*To whom correspondence should be addressed: Email: liu.liping@rutgers.edu (L.L.); psharma@uh.edu (P.S.)
Edited By Cristina Amon

Abstract

The classical Ginzburg–Landau model has long provided the foundation for modeling superconductivity, yet it does not fully capture the rich diversity of unconventional superconducting phenomena observed experimentally. Examples include magnetic superconductors, re-entrant superconductivity, and the cuprates—materials whose behaviors are not adequately explained by traditional Ginzburg–Landau and/or Bardeen–Cooper–Schrieffer (BCS) theories. In this work, we develop a thermodynamically consistent reformulation of the Ginzburg–Landau theory expressed in gauge-invariant variables. This framework, when extended to anisotropic settings, naturally predicts preferential domain orientations and, crucially, reveals a previously overlooked symmetry-allowed term that breaks time-reversal symmetry. Such a term is essential for capturing the behavior of magnetic superconductors, particularly antiferromagnetic systems where superconductivity and magnetism coexist. We further demonstrate that stabilization of antiferromagnetic superconducting states necessitates a loss of convexity in the free energy. Together, these results unify disparate phenomena within a single-component order parameter and offer a systematic route for understanding, modeling, and controlling unconventional superconducting states.

Keywords unconventional superconductivity, antiferromagnetic superconductor, Thermodynamics, Quantum Materials

Significance statement

The classical Ginzburg–Landau theory struggles to explain unconventional behaviors such as the coexistence of superconductivity with magnetism or the preferred domain orientations. We present a reformulation using gauge-invariant variables that reveals a previously overlooked symmetry-allowed term. This approach naturally predicts the paradoxical coexistence of antiferromagnetism and superconductivity while also explaining direction-dependent surface energies in anisotropic materials. By unifying these phenomena within a single-component order parameter, this work provides a simple and powerful tool for designing and understanding complex quantum materials.

Introduction

The macroscopic behavior of superconductors is well captured by the Ginzburg–Landau (GL) theory, a cornerstone of condensed matter physics that exemplifies how emergent continuum order parameters unravel complex quantum phenomena (1, 2). The theory successfully explains several key features of observable superconductor behavior, such as the Meissner effect (1, 3, 4), phase transition (4, 5), jump in specific heat capacity (4, 6–8), the existence of a critical magnetic field (4), intermediate state microstructure (9) (with theoretical predictions (2, 10–16) and experimental validation (17–21)), vortices (18, 22–26), and surface energy (27–29), among others (30–35).

In this article, we revisit the Ginzburg–Landau theory of superconductivity by reformulating it in terms of *gauge-invariant*

Received: December 23, 2025. **Accepted:** April 17, 2026

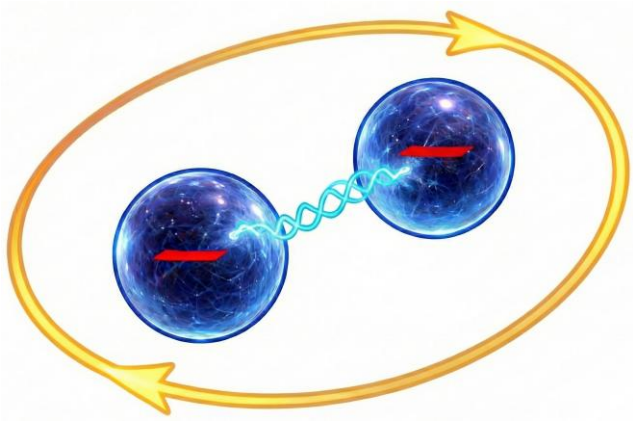

Figure 1 Schematic showing a rotating Cooper pair, illustrating a possible microscopic mechanism for Cooper pair formation. The rotation of the paired electrons about their common center of mass provides a natural means for generating a magnetic field, suggesting how superconductivity and magnetism may coexist within a unified microscopic picture.

variables. In its simplest extension, this approach permits the treatment of material parameters independently of their quantum mechanical origins, as otherwise would be suggested by Gorkov's linkage between Bardeen–Cooper–Schrieffer (BCS) theory and Ginzburg–Landau. Notably, this reformulation predicts domain wall anisotropy with preferred orientations. Furthermore, it reveals the absence of a time reversal symmetry breaking (TRSB) term that is permitted in certain magnetic crystals and thus allows the superconducting state to coexist with magnetism. One possible microscopic mechanism underlying TRSB is that of rotating Cooper pairs (see Fig. 1), where rotation about an axis can generate a magnetic field. However, in this work, we adopt a macroscopic thermodynamic perspective and do not rely on a specific microscopic model or its detailed connection to the proposed coupling term. Our position is that being allowed by symmetry and its predictions being observed in real material is sufficient justification. The interested reader should read up on this rich subject from any number of available resources; we present a few (36–38). This term was first identified by Gurtin (39), although his contribution appears to have been largely overlooked. We incorporate this missing term and investigate its consequences. In the isotropic embodiment of our formulation, we find that the ensuing solutions can be mapped back onto those of the standard isotropic Ginzburg–Landau theory. This suggests that, for isotropic solids, the modifications do not lead to any observable differences, potentially explaining why it has remained unnoticed. However, in the anisotropic setting, our formulation diverges from the classical anisotropic Ginzburg–Landau model. Specifically, we uncover new nontrivial solutions with two key physical implications:

(i) Direction-dependent surface energy.
(ii) Coexistence of superconductivity and magnetism for crystals that break time-reversal symmetry.

For magnetic fields applied along a crystallographic axis in materials possessing orthorhombic symmetry or higher, the anisotropic Ginzburg–Landau theory predicts that the surface energy is independent of domain-wall orientation within the plane perpendicular to the applied field (see Section S5 in the Supplementary material). In contrast, our reformulation introduces a directional dependence, representing a fundamental departure from the classical theory. When the surface energy is positive in all directions, the resulting domain morphology exhibits a preferred orientation, consistent with anisotropic interfacial energetics. Conversely, if the surface energy is negative along specific directions, the system favors the formation of laminates that increase the interfacial area along those directions to reduce the total energy.

Motivated by the experimentally observed phenomenon of the coexistence of superconductivity and magnetism at zero external field (40–42), we seek solutions by adding the TRSB term. The reason for this is 2-fold. First, the standard Ginzburg–Landau at zero external field predicts perfect diamagnetism along with zero resistance. Second, the TRSB term is what would give rise to magnetism. The TRSB superconducting phase is supported by experimental observations from Kerr rotation (43–45), small-angle neutron scattering (SANS) (41), and μSR spectroscopy (46). We present an instability-based argument showing that such coexisting states are energetically preferred over the homogeneous superconducting phase in the absence of an external field.

Reformulation of the Ginzburg–Landau model for the isotropic case

We begin by considering the isotropic Ginzburg–Landau formulation. The isotropic Ginzburg–Landau formulation describes superconductivity in a domain $\Omega \subset \mathbb{R}^3$ under an external magnetic field $\underline{H}$. It involves a complex order parameter $\psi : \Omega \to \mathbb{C}$ and a magnetic vector potential $\underline{A} : \mathbb{R}^3 \to \mathbb{R}^3$. The equilibrium configuration minimizes the Helmholtz free energy,

$$\mathcal{GL}[\psi, \underline{A}; \underline{H}] := \int_\Omega \frac{\hat{\beta}}{2}\left(|\psi|^2 + \frac{\hat{\alpha}}{\hat{\beta}}\right)^2 + \frac{1}{2m^*}\left|\frac{\hbar}{i}\nabla\psi - \frac{e^*}{c}\underline{A}\psi\right|^2 \mathrm{d}x + \frac{1}{8\pi}\int_{\mathbb{R}^3} |\mathrm{curl}\underline{A} - \underline{H}|^2 \,\mathrm{d}x, \tag{1}$$

where $\hat{\alpha}$ is temperature-dependent, switching sign at T_c, and $\hat{\beta} > 0$ ensures stability. The equilibrium configuration is determined by solving the minimization problem:

$$\inf_{\psi, \underline{A} \in \mathcal{A}_1} \mathcal{GL}[\psi, \underline{A}; \underline{H}], \quad \mathcal{A}_1 := \{\psi, \underline{A} \text{ are such (1) is well-defined}\}. \tag{2}$$

In particular, curl$\underline{A}$ represents magnetic fields, leading to the continuity condition $[\![\underline{A}]\!] \times n = 0$ at interfaces (33).

To reformulate in real variables, we express $\psi = ue^{i\theta}$, where $u = |\psi|$ and θ is the phase. The gauge-invariant vector potential $\underline{A}_0 = \underline{A} - (\hbar c/e^*)\nabla\theta$ transforms the energy into

$$\tilde{\mathcal{GL}}[u, \theta, \underline{A}; \underline{H}] := \int_\Omega \frac{\hat{\beta}}{2}\left(u^2 + \frac{\hat{\alpha}}{\hat{\beta}}\right)^2 + \frac{\hbar^2}{2m^*}(\nabla u)^2 + \frac{e^{*2}}{2m^* c^2}u^2\underline{A}_0^2 \,\mathrm{d}x + \int_{\mathbb{R}^3} \frac{|\mathrm{curl}\,\underline{A} - \underline{H}|^2}{8\pi}\,\mathrm{d}x. \tag{3}$$

The minimization problem associated with

$$\inf_{(u,\theta,\underline{A}) \in \underline{\mathcal{A}}_2} \tilde{\mathcal{GL}}[u, \theta, \underline{A}; \underline{H}], \quad \mathcal{A}_2 := \{u, \theta, \underline{A} | u \geq 0, (3) \text{ is well-defined}\}, \tag{4}$$

where $\mathcal{A}_2$ denotes the class of admissible functions. We note that the traditional Ginzburg–Landau parameters α and β have been relabeled as $\hat{\alpha}$ and $\hat{\beta}$ in the present formulation. This change is made for notational clarity, as the symbols α and β are later reserved (see Loss of stability section) to denote the sine and cosine of an angle.

To simplify further, we nondimensionalize (3). We set $\underline{x}' = \underline{x}/\lambda$ and $u_\infty^2 = |\hat{\alpha}|/\hat{\beta}$. Another point to notice is that in the first quadratic term, we have something that looks like u_∞^2. However, since $\hat{\alpha}$ changes sign with T, we will set $(u^2 + \hat{\alpha}/\hat{\beta})^2 = (u^2 \pm u_\infty^2)^2$. The reasoning is that we choose the $+$ sign for $T > T_c$ and the $-$ sign for $T < T_c$. We transform all the terms to get,

$$\lambda^3 u_\infty^2 |\hat{\alpha}| \left[\int_{\Omega/\lambda} \frac{(1 \pm u'^2)^2}{2} + \frac{(\nabla' u')^2}{\kappa^2} + \frac{e^{*2}}{2|\hat{\alpha}| m^* c^2} u'^2 \underline{A}_0^2 + \int_{\mathbb{R}^3} \frac{|\mathrm{curl}' \underline{A} - \lambda \underline{H}|^2}{8\pi \lambda^2 u_\infty^2 |\hat{\alpha}|} \right], \tag{5}$$

where in the above, we have set $\kappa = \lambda/\xi$, $\xi = \hbar^2/2m^*|\hat{\alpha}|$ and $u' = u/u_\infty$. Now note that we can set the coefficients of the two $\underline{A}$ terms equal to get the following relation $\lambda^2 = m^* c^2/4\pi u_\infty^2 e^{*2}$; this is the magnetic penetration depth. We can therefore set $\underline{A}'_0 = \underline{A}_0/\sqrt{8\pi\lambda^2 u_\infty^2 |\hat{\alpha}|}$ and define $\underline{H}' = \underline{H}\sqrt{\hat{\beta}/8\pi\hat{\alpha}^2}$. Moreover, the energy density can be scaled by $\lambda^3 u_\infty^2 |\hat{\alpha}|$. Then, we can write down the nondimensional energy density as

$$\hat{GL}[u', \underline{A}', \theta; \underline{H}] := \int_{\Omega'} \frac{\left(1 \pm u'^2\right)^2}{2} + \frac{(\nabla' u')^2}{\kappa^2} + u'^2 \underline{A}'^2_0 + \int_{\mathbb{R}^3} |\mathrm{curl}' \underline{A}' - \underline{H}'|^2, \tag{6}$$

where $\Omega' = \Omega/\lambda$. Dropping the primes and setting $u = 0$ for the normal phase and $u = 1$ for superconductivity. The resulting functional is

$$\hat{GL}[u, \underline{A}, \theta, T; \underline{H}] := \int_\Omega \frac{\left(1 \pm u^2\right)^2}{2} + \frac{(\nabla u)^2}{\kappa^2} + u^2 \underline{A}_0^2 \, \mathrm{d}x + \int_{\mathbb{R}^3} |\mathrm{curl} \underline{A} - \underline{H}|^2 \, \mathrm{d}x, \tag{7}$$

where we use "+" for $T > T_c$ and "−" otherwise. The minimization problem can be written as

$$\inf_{(u,\theta,\underline{A}) \in \mathcal{A}_2} \hat{GL}[u, \underline{A}, \theta, T; \underline{H}]. \tag{8}$$

For $T > T_c$, the minimizer is $u = 0$, with $\mathrm{curl}\underline{A} = \underline{H}$, corresponding to the normal state. Below T_c, superconductivity emerges, and the functional simplifies to depend only on κ, the Ginzburg–Landau parameter. We use this formulation moving forward.

We now advance the classical isotropic Ginzburg–Landau functional by introducing a critical extension—an additional term representing the cross-coupling between the second and third terms in (3). This modification was first noticed by Gurtin (39).[a] The resulting energy in dimensional form is given by

$$\mathcal{GL}_G[u, \underline{A}, \theta; \underline{H}] := \int_\Omega \frac{\hat{\beta}}{2} \left(u^2 + \frac{\hat{\alpha}}{\hat{\beta}} \right)^2 + \tilde{\tau}_1 (\nabla u)^2 + \tilde{\tau}_2 u \nabla u \cdot \underline{A}_0 + \tilde{\tau}_3 u^2 \underline{A}_0^2 \, \mathrm{d}x + \int_{\mathbb{R}^3} \frac{|\mathrm{curl}\underline{A} - \underline{H}|^2}{8\pi} \, \mathrm{d}x. \tag{9}$$

Upon nondimensionalization,

$$\hat{GL}_G[u, \underline{A}, \theta; \underline{H}] = \int_\Omega \frac{1}{2}\left(1 - u^2\right)^2 + \frac{(\nabla u)^2}{\kappa^2} + \tau_2 u \nabla u \cdot \underline{A}_0 + u^2 \underline{A}_0^2 \, \mathrm{d}x + \int_{\mathbb{R}^3} |\mathrm{curl}\underline{A} - \underline{H}|^2 \, \mathrm{d}x. \tag{10}$$

This modification does not emerge from the original formulation in (1), but becomes inevitable when the theory is reformulated in terms of gauge-invariant variables. Notice that this term is odd in A_0. This means that this term/model is only applicable to a TRSB material; hinting at the material being magnetic.

Crucially, this term is fully consistent with the symmetries of the problem and, as such, must have a nontrivial impact on the properties of some superconductors that satisfy the requisite symmetry constraints.

The inclusion of this term raises a natural and pressing question: Does our modification give rise to any new phenomenology? Although nonconvexity alone does not ensure the existence of new solutions, it often signals the possibility of phase transitions and rich variational structure. Our extension renders the energy landscape explicitly nonconvex, while maintaining structural simplicity. It modifies the test-function space $(\nabla u, \underline{A}_0 u)$ by deforming circular energy contours into ellipses—subtly altering the geometry without destroying the foundational features of the model. This balance of generality, symmetry compliance, and mathematical tractability makes our modification a compelling and essential step in extending the classical Ginzburg–Landau framework.

Despite modifying the free energy landscape, the presence of τ_2 does not introduce fundamentally new solutions. To see this, consider the substitution:

$$(u, A, \theta) \mapsto (u, R = A + \nabla \ln u^{\tau_2/2}, \theta). \tag{11}$$

With this substitution, we can map (10) to (7) with an effective Ginzburg–Landau parameter, $1/\kappa_{\mathrm{eff}}^2 = 1/\kappa^2 - \tau_2^2/4$. Thus, the minimizers of the latter can be used to determine the minimizers of the former using the reverse mapping.

Thermodynamic reformulation in the anisotropic setting

To observe nontrivial consequences of our modification, it is necessary to work within the anisotropic framework. We begin by considering the anisotropic Ginzburg–Landau model, which generalizes the isotropic case through the introduction of an effective mass tensor $\underline{\underline{M}}_S$, leading to the following free energy functional:

$$\mathcal{GL}_A[\psi, \underline{A}; \underline{H}] := \int_\Omega \frac{\hat{\beta}}{2} \left(|\psi|^2 + \frac{\hat{\alpha}}{\hat{\beta}} \right)^2 + \frac{1}{2} \left(-i\hbar\nabla + \frac{e^* \underline{A}}{c} \right) \psi^* \cdot M_S^{-1} \left(i\hbar\nabla + \frac{e^* \underline{A}}{c} \right) \psi \, \mathrm{d}x + \frac{1}{8\pi} \int_{\mathbb{R}^3} |\mathrm{curl}\underline{A} - \underline{H}|^2 \, \mathrm{d}x, \tag{12}$$

Setting $M_S^{-1} = \underline{\underline{M}}^{-1}/m^*$ and rewriting in polar form, the functional becomes

$$\begin{aligned}\mathcal{GL}_A[u, \underline{A}, \theta; \underline{H}] : = \int_\Omega \frac{\left(1-u^2\right)^2}{2} + \frac{\nabla u}{\kappa} \cdot \underline{\underline{M}}^{-1} \frac{\nabla u}{\kappa} \\ + u^2 \underline{A}_0 \cdot \underline{\underline{M}}^{-1} \underline{A}_0 \, \mathrm{d}x + \int_{\mathbb{R}^3} |\mathrm{curl}\underline{A} - \underline{H}|^2 \, \mathrm{d}x.\end{aligned} \tag{13}$$

To introduce the anisotropic version of our modification, we generalize the scalar coefficients in (9) to tensors,[b] obtaining

$$\begin{aligned}GL_{A,G}[u, \theta, \underline{A}; \underline{H}] : = \int_\Omega \frac{(1-u^2)^2}{2} + \nabla u \cdot \underline{\underline{K}}_m \nabla u \\ + 2\underline{\underline{T}}_m \nabla u \cdot \underline{A}_0 u + u^2 \underline{A}_0 \cdot \underline{\underline{M}}_m \underline{A}_0 \, \mathrm{d}x \\ + \int_{\mathbb{R}^3} |\mathrm{curl}\underline{A} - \underline{H}|^2 \, \mathrm{d}x,\end{aligned} \tag{14}$$

where in the above, we have replaced $\underline{\underline{M}}^{-1}/\kappa^2$ with $\underline{\underline{K}}_m$, we introduce a tensorial version of the τ_2 term from (10) and finally $\underline{\underline{M}}^{-1}$ has been replaced by $\underline{\underline{M}}_m$ for ease of notation. The Euler Lagrange equations associated with the above functional are given by,

$$\begin{aligned}&-u + u^3 - \mathrm{div}\,(\underline{\underline{T}}_m^T \underline{A}_0)u + u\underline{A}_0 \cdot \underline{\underline{M}}_m \underline{A}_0 = \mathrm{div}\,(\underline{\underline{K}}_m \nabla u) \quad \text{in } \Omega \\ &\underline{\underline{K}}_m \nabla u \cdot n + \underline{\underline{T}}_m^T \underline{A}_0 u \cdot n = 0 \quad \text{on } \partial\Omega \\ &\mathrm{curl}\ \mathrm{curl}\ \underline{A} + \underline{\underline{T}}_m u \nabla u + u^2 \underline{\underline{M}}_m \underline{A}_0 = 0 \quad \text{in } \Omega \\ &\mathrm{curl}\ \mathrm{curl}\ \underline{A} = 0 \quad \text{in } \Omega^c \\ &[\![\underline{A}]\!] \times n = 0 \quad \text{on } \partial\Omega \\ &[\![\mathrm{curl}\ \underline{A} - \underline{H}]\!] \times n = 0 \quad \text{on } \partial\Omega.\end{aligned} \tag{15}$$

Notice that the functional (14) is gauge invariant with $u = 0$, $\mathrm{curl}\underline{A} = \underline{H}$ (normal phase) and $u = 1$, $\underline{A}_0 = 0$ (superconducting phase) being critical points. In Section S1 of the Supplementary material, we show that these correspond to the solutions under zero field and high field, respectively.

For analytical solutions, we consider a prismatic domain aligned with a uniform applied field $\underline{H}$. If $\underline{\underline{K}}_m \underline{H}$, $\underline{\underline{T}}_m \underline{H}$, $\underline{\underline{M}}_m \underline{H} \parallel \underline{H}$, the problem reduces to a 2D formulation perpendicular to $\underline{H}$. Details are available in the Section S4 in the Supplementary material. Many crystal structures, including monoclinic, satisfy this condition.

Given the ansatz above, we consider the surface energy for 1D domain walls. Our tensor modification introduces effects absent in traditional Ginzburg–Landau theory, notably the dependence of domain wall surface energy on orientation. To analyze this, we first examine the special case where $\underline{\underline{T}}_m = 0$ in (14). The surface energy is then computed as a function of domain wall direction. Once obtained, the equilibrium domain shape follows from the Wulff construction (47, 48). We then consider the special case of $\underline{\underline{T}}_m \neq 0$ and show that this can lead to antiferromagnetic (AFM) superconductors.

Direction dependent surface energy

We first consider the case $\underline{\underline{T}}_m = 0$ in (14). Assuming orthorhombic crystal symmetry (see Section S3 in the Supplementary material for effect of crystal symmetry) with the applied field along the a, b, or c-axis, the problem reduces to two dimensions (see Theorem 2 in Section S4 in Supplementary material for proof of problem reducing to 2D). Setting $\underline{\underline{M}}_m = \underline{\underline{I}}$ (without loss of generality) and assuming infinite domain, the Euler–Lagrange equations simplify to

$$\begin{aligned}-u + u^3 + u\underline{A}_0^2 = \mathrm{div}\,(\underline{\underline{K}}_m \nabla u) \quad &\text{in} \quad \mathbb{R}^2 \\ \mathrm{curl}\ \mathrm{curl}\ \underline{A} + u^2 \underline{A}_0 = 0 \quad &\text{in} \quad \mathbb{R}^2.\end{aligned} \tag{16}$$

Note that for fields applied along a crystal axis of orthorhombic symmetry or higher, we can show that the anisotropic Ginzburg–Landau theory maps onto the isotropic case via a change of variables (49), preserving direction-independent surface energy (see Section S5 in the Supplementary material for proof). In such a case, since the surface energy is identical for all orientations, there is no energetic preference for any particular domain-wall direction, and the resulting laminate structures are expected to form along arbitrary orientations, as commonly observed in classical intermediate-state patterns. However, our modification breaks this invariance, introducing a directional dependence on surface energy. This suggests that the domain walls have a preferential directional dependence.

To study surface energy versus domain wall direction, we assume $\Omega = \mathbb{R}^2$ and consider the following ansatz for the minimizers:

$$u(\underline{x}) = \hat{u}(\underline{x} \cdot \underline{d}), \quad \underline{A}(\underline{x}) = \underline{\hat{A}}(\underline{x} \cdot \underline{d}), \quad \theta(\underline{x}) = 0, \tag{17}$$

where $\underline{d} \in S^1$ denotes the direction normal to the domain wall—the direction along which the superconducting order parameter varies.

In this subsection, we will analyze the surface energy calculation. Out starting point is the functional (14) with test functions (17):

$$\begin{aligned}GL_{A,G}[\hat{u}, 0, \underline{\hat{A}}; H] : = \int_\Omega \frac{(1-\hat{u}^2)^2}{2} + K_1(\hat{u}')^2 + \hat{u}^2 \underline{\hat{A}}^2 \, \mathrm{d}s \\ + \int_{\mathbb{R}^2} |\underline{d} \times \underline{\hat{A}}' - H|^2 \, \mathrm{d}s,\end{aligned} \tag{18}$$

where $K_1 = \underline{d} \cdot \underline{\underline{K}}_m \underline{d}$ and $s = \underline{x} \cdot \underline{d}$.

For numerical tractability, we restrict the domain to $L_x \times L_y$ and rescale length along $\underline{d}$ to L_x. Under this assumption, the problem simplifies to

$$\begin{aligned}GL_{A,G}[\hat{u}, 0, \underline{\hat{A}}; \underline{H}] : = L_y \int_{[0,L_x]} \frac{(1-\hat{u}^2)^2}{2} + K_1(\hat{u}')^2 + \hat{u}^2 \underline{\hat{A}}^2 \\ + |\underline{d} \times \underline{\hat{A}}' - \underline{H}|^2 \, \mathrm{d}s \\ \text{subject to} \ : \ \hat{u}(0) = 0, \quad \hat{u}(L_x) = 1, \\ \underline{\hat{A}}'(0) = \underline{d}_\perp H, \quad \underline{\hat{A}}(L_x) = 0,\end{aligned} \tag{19}$$

where we set $\underline{\hat{A}} = \underline{d}_\perp Hs$ in Ω^c to reduce the problem from $\mathbb{R}^2$ to $[0, L_x] \times [0, L_y]$. Here, $\underline{d}_\perp$ is the counter-clockwise rotated component of $\underline{d}$. The boundary conditions help us get a domain wall by transitioning from the normal (at 0) to the superconducting phase (at L_x).

Substituting the domain-wall ansatz (17) into the Euler–Lagrange equations (15) with $\underline{\underline{T}}_m = 0$, we recover the isotropic Ginzburg–Landau domain-wall formulation, with the Ginzburg–Landau parameter κ replaced by the anisotropic coefficient K_1. Since K_1 depends on the orientation $\underline{d}$, the corresponding interfacial energy inherits this directional dependence. Consequently, the equilibrium domain-wall orientation is governed by the minimization of this anisotropic surface energy, a feature absent in the conventional isotropic theory.

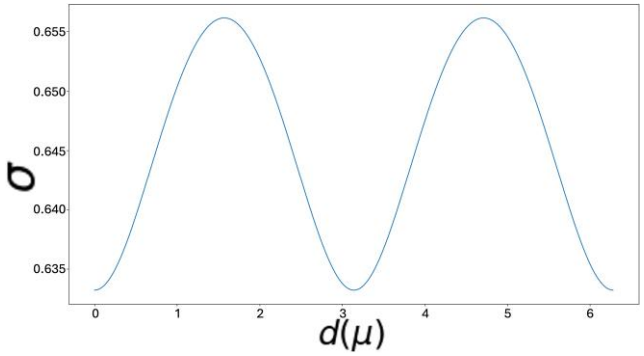

Figure 2 Plot of the surface energy versus direction of the domain wall. The domain wall direction is parameterized by the angle μ, so $\underline{d} = (\cos\mu,\ \sin\mu)$. We chose $(\underline{\underline{K}}_m)_{11} = 1$, $(\underline{\underline{K}}_m)_{12} = 0.0$, $(\underline{\underline{K}}_m)_{22} = 4.0$.

The numerical results, shown in Fig. 2, clearly demonstrate that the surface energy varies with the orientation of the domain wall. In contrast to the conventional anisotropic Ginzburg–Landau theory, where the surface energy is independent of direction, our formulation naturally predicts a preferred domain-wall orientation. When the surface energy remains positive for all orientations, the equilibrium domain morphology follows from the Wulff construction (47, 48).

We can further consider the special case with $\underline{\underline{K}}_m = \mathrm{diag}(K_{11}, K_{22})$, with $K_{11} \ll 1$ and $K_{22} \gg 1$. In this situation, the system exhibits type I behavior along x_1 and type II behavior along x_2 (see Section 2.4 in (27)). Since surface energy is positive for type I and negative for type II (27–29), it varies continuously with orientation. As a result, domain walls favor elongation along x_2, preferring laminate solutions.

Loss of stability

For the functional (14), to ensure that it reproduces the standard results of Ginzburg–Landau—namely, normal to superconducting phase transition at zero external field across the transition temperature—it is necessary that the tensor Γ be positive definite.

$$f \cdot \Gamma f = f \cdot \begin{pmatrix} \underline{\underline{K}}_m & \underline{\underline{T}}_m^T \\ \underline{\underline{T}}_m & \underline{\underline{M}}_m \end{pmatrix} f > 0 \quad \forall\ f \in S^5. \tag{20}$$

We show in Section S1 in the Supplementary material that, for $H = 0$ and a positive definite Γ (see Section S2 in the Supplementary material), the global minimizer corresponds to $u = 1$ and $\underline{A}_0 = 0$. Hence, in the absence of an applied magnetic field, antiferromagnetic superconductivity cannot emerge unless the free energy loses convexity. The natural question, then, is how such a loss of convexity may occur.

A key outcome of the above analysis is that the emergence of antiferromagnetic superconducting states is directly tied to the loss of convexity of the free energy functional. In particular, the coupled system reduces to a single nonlinear equation characterized by the parameter c (depends on $\underline{\underline{K}}_m$, $\underline{\underline{T}}_m$, *and* $\underline{\underline{M}}_m$). Linearization about the uniform superconducting state reveals that oscillatory (spatially modulated) solutions arise when $c < 0$, which corresponds to the condition:

$$(\underline{e} \cdot \underline{\underline{T}}_m \underline{d})^2 > (\underline{d} \cdot \underline{\underline{K}}_m \underline{d})\ (\underline{e} \cdot \underline{\underline{M}}_m \underline{e}),$$

which is opposite of the inequality derived for convexity in Section S2 of the Supplementary material. This condition provides a clear and explicit criterion for the loss of convexity of Γ driven by sufficiently strong TRSB coupling. Beyond this threshold, the homogeneous superconducting state becomes unstable to oscillatory perturbations, leading to spatial variations in both the order parameter and magnetic field, and thereby stabilizing an antiferromagnetic superconducting phase.

To investigate this, we perform a stability analysis about the uniform superconducting state at $H = 0$, ie $(u, \underline{A}) = (1, 0)$, and identify the conditions under which the system becomes unstable, thereby favoring the emergence of an antiferromagnetic superconducting phase. The starting point for our analysis is the following 1D Ansatz:

$$u(\underline{x}) = \hat{u}(\underline{x} \cdot \underline{d}), \quad \underline{A}(\underline{x}) = \hat{A}(\underline{x} \cdot \underline{d})\underline{e}, \quad \theta = 0, \tag{21}$$

where $\underline{d}, \underline{e} \in S^1$ are arbitrary. We moreover set $\underline{x} \cdot \underline{d} = s$. Substituting into (15) and considering an infinite domain, we get

$$\begin{gathered} -u + u^3 - (\underline{d} \cdot \underline{\underline{T}}_m^T \underline{e})A'u + (\underline{e} \cdot \underline{\underline{M}}_m \underline{e})uA^2 = (\underline{d} \cdot \underline{\underline{K}}_m \underline{d})u'' \\ A''\left((\underline{d} \cdot \underline{e})\underline{d} - \underline{e}\right) + (\underline{\underline{T}}_m \underline{d})uu' + (\underline{\underline{M}}_m \underline{e})u^2 A = 0, \end{gathered} \tag{22}$$

where in the above formulation, we have taken $\underline{\underline{M}}_m = \underline{\underline{I}}$. This choice can always be achieved by an appropriate rescaling, provided that $\underline{\underline{M}}_m$ is positive definite. It is important to note that, since our interest lies in the loss of convexity of Γ as a mechanism for stabilizing an antiferromagnetic phase, one might consider the special case in which $\underline{\underline{M}}_m$ or $\underline{\underline{K}}_m$ itself loses positive definiteness leading to loss of positive definiteness of Γ. We are specifically interested in the loss of positive definiteness of Γ without loss of positive definiteness of $\underline{\underline{K}}_m$ or $\underline{\underline{M}}_m$. This involves $\underline{\underline{T}}_m$ being large which in turn implies large TRSB effects.

Taking the inner product with respect to $\underline{d}$ for (22)(b), gives us the relation, $A = -\frac{T_2}{\beta}(\ln u)'$, where $\beta = \underline{d} \cdot \underline{e}$ and $T_2 = \underline{d} \cdot \underline{\underline{T}}_m \underline{d}$. We used the fact that $u \neq 0$ identically. This yields the following 1D system:

$$\begin{gathered} -u + u^3 - T_1 A'u + uA^2 = K_1 u'', \\ -\alpha^2 A'' + T_1 uu' + u^2 A = 0, \\ T_2 uu' + \beta u^2 A = 0, \end{gathered} \tag{23}$$

where $\beta = \underline{d} \cdot \underline{e}$, $T_2 = \underline{d} \cdot \underline{\underline{T}}_m \underline{d}$, $T_1 = \underline{e} \cdot \underline{\underline{T}}_m \underline{d}$, $K_1 = \underline{d} \cdot \underline{\underline{K}}_m \underline{d}$, and $\alpha = \underline{d} \times \underline{e}$. The derivatives are with respect to the argument, and we have dropped the hats for brevity. It is worth noting that the α and β mentioned above are not related to $\hat{\alpha}$ and $\hat{\beta}$ appearing in (1) and (3). We are interested in doing a stability analysis to show that the system loses convexity. This is because loss of convexity will allow for a different state to have lower energy. We want to consider the situation when this loss of convexity leads to an antiferromagnetic state. To this end, we will perform a stability analysis to determine the conditions under which antiferromagnetic state is preferred. The motivation here is that instabilities often lead to oscillatory modes. An oscillatory u will lead to an oscillatory $\underline{A}$, which would lead to an oscillatory curl$\underline{A}$. The key point is that the oscillation for curl$\underline{A}$ will be about 0.

Notice that (23)(c) yields a closed expression for A (for $\beta \neq 0$):

$$A = -\frac{T_2}{\beta}\frac{u'}{u}, \quad A' = -\frac{T_2}{\beta}\left(\frac{u''}{u} - \frac{u'^2}{u^2}\right), \quad A^2 = \left(\frac{T_2}{\beta}\right)^2 \frac{u'^2}{u^2}. \tag{24}$$

Eliminating A from (23)(a) yields,

$$K_1 u'' = -u + u^3 + T_1 \frac{T_2}{\beta}\left(u'' - \frac{u'^2}{u}\right) + \left(\frac{T_2}{\beta}\right)^2 \frac{u'^2}{u}, \tag{25}$$

or, equivalently,

$$\left(K_1 - \frac{T_1 T_2}{\beta}\right) u'' = -u + u^3 + \left(-\frac{T_1 T_2}{\beta} + \frac{T_2^2}{\beta^2}\right)\frac{u'^2}{u}. \tag{26}$$

Using (23)(c), we get the following expression:

$$A'' = -\frac{T_2}{\beta}\left(\frac{u'''}{u} - \frac{3u'u''}{u^2} + \frac{2u'^3}{u^3}\right). \tag{27}$$

Substituting into (23)(b) yields the u-only third-order equation,

$$\frac{\alpha^2 T_2}{\beta}\left(\frac{u'''}{u} - \frac{3u'u''}{u^2} + \frac{2u'^3}{u^3}\right) + \left(T_1 - \frac{T_2}{\beta}\right) u u' = 0 \tag{28}$$

whose first integral is

$$\frac{\alpha^2 T_2}{\beta}\left(\frac{u''}{u} - \frac{u'^2}{u^2}\right) + \frac{T_1 - \frac{T_2}{\beta}}{2} u^2 = C \tag{29}$$

and, equivalently,

$$\frac{\alpha^2 T_2}{\beta}\left(u'' - \frac{u'^2}{u}\right) + \frac{T_1 - \frac{T_2}{\beta}}{2} u^3 = C u \tag{30}$$

We thus have two equations in u. This is an overdetermined system. One way this can be a solution is if both equations are not independent. We introduce $q = \ln u$ so that $\frac{u'}{u} = q'$ and $\frac{u''}{u} - (\frac{u'}{u})^2 = q''$. Substituting $u = e^q$ into (26) yields,

$$\left(K_1 - \frac{T_1 T_2}{\beta}\right) q'' = -1 + e^{2q} + \left(\frac{T_2^2}{\beta^2} - K_1\right)(q')^2 \tag{31}$$

while substituting $u = e^q$ into (30) yields,

$$\alpha^2 \frac{T_2}{\beta} q'' + \frac{T_1 - \frac{T_2}{\beta}}{2} e^{2q} = C. \tag{32}$$

Comparing (31) and (32), we see that the $(q')^2$–term must vanish. This gives us the condition,

$$K_1 = \frac{T_2^2}{\beta^2}. \tag{33}$$

At first glance, this condition may appear overly restrictive. However, it is important to recall that the coefficients K_1, T_2, and β depend explicitly on the material tensors $\underline{\underline{K}}_m$ and $\underline{\underline{T}}_m$, as well as on the chosen directions $\underline{d}$ and $\underline{e}$. For a given material, the tensors $\underline{\underline{K}}_m$ and $\underline{\underline{T}}_m$ are fixed, while the directions ($\underline{d}$, $\underline{e}$) are free to adjust. The system may therefore select directions that satisfy (33), effectively relaxing the constraint and rendering it considerably less restrictive than it may initially appear.

We now demand (31) be a scalar multiple of (32), ie $\lambda\times$ (32) = (31), determines

$$\lambda\alpha^2\sqrt{K_1} = K_1 - T_1\sqrt{K_1}, \quad \lambda\left(\frac{T_1 - \sqrt{K_1}}{2}\right) = -1, \quad \lambda C = -1, \tag{34}$$

hence

$$\lambda = \frac{2}{\sqrt{K_1} - T_1}, \quad \alpha^2 = \frac{(\sqrt{K_1} - T_1)^2}{2}. \tag{35}$$

We define the parameter,

$$c = K_1 - \frac{T_1 T_2}{\beta} = \sqrt{K_1}\left(\sqrt{K_1} - T_1\right). \tag{36}$$

Then, (31) and (32) collapse to the single nonlinear ordinary differential equation

$$c q'' + \left(1 - e^{2q}\right) = 0 \tag{37}$$

We can now perform stability analysis by linearizing about $u = 1 \equiv q = 0$. Using $e^{2q} = 1 + 2q + O(q^2)$, we obtain the linearized oscillator

$$c q'' - 2q = 0 \tag{38}$$

so that oscillatory solutions require $c < 0$.

Material selection for oscillatory (AFM) states

We will proceed with a general form for the material tensor and simplify the calculations by picking $\underline{d} = (1, 0)$ and let

$$\underline{\underline{K}}_m = \begin{pmatrix} K_{11} & K_{12} \\ K_{12} & K_{22} \end{pmatrix}, \quad \underline{\underline{T}}_m = \begin{pmatrix} T_{11} & T_{12} \\ T_{21} & T_{22} \end{pmatrix}, \quad \Gamma = \begin{pmatrix} \underline{\underline{K}}_m & \underline{\underline{T}}_m \\ \underline{\underline{T}}_m^T & \underline{\underline{I}} \end{pmatrix}. \tag{39}$$

Recall the constants $K_1 = \underline{d}\cdot\underline{\underline{K}}_m\underline{d} = K_{11}$ and $T_2 = \underline{d}\cdot\underline{\underline{T}}_m\underline{d} = T_{11}$, while $\beta = \cos\theta$. We restrict ourselves to Orthorhombic symmetry. This means that in the principal frame $\underline{\underline{K}}_m$ and $\underline{\underline{T}}_m$ are diagonal. Thus in any other frame, they will be symmetric. This suggests that $T_{21} = T_{12}$. From (33):

$$\begin{aligned} &\beta = \cos\theta = \tilde{\mu}\tfrac{T_{11}}{\sqrt{K_{11}}}, \\ &\underline{e} = (\cos\theta,\ \sin\theta) = \left(\tilde{\mu}\tfrac{T_{11}}{\sqrt{K_{11}}}, \tilde{\nu}\sqrt{1 - \tfrac{T_{11}^2}{K_{11}}}\right), \end{aligned} \tag{40}$$

where $\tilde{\mu}, \tilde{\nu} \in \pm 1$. Moreover note that $\tilde{\mu} = \mathrm{sgn}(T_{11}\beta)$. This is because $K_{11} > 0$.

This gives us

$$T_1 = \underline{e}\cdot\underline{\underline{T}}_m\underline{d} = \frac{\tilde{\mu}T_{11}^2 + \tilde{\nu}T_{21}\sqrt{K_{11} - T_{11}^2}}{\sqrt{K_{11}}}. \tag{41}$$

Using (35) with $\alpha = \sin\theta = \tilde{\nu}\sqrt{\frac{K_{11} - T_{11}^2}{K_{11}}}$ gives

$$\alpha = \tilde{\xi}\frac{\sqrt{K_1} - T_1}{\sqrt{2}} \Longrightarrow T_1 = \sqrt{K_{11}} - \tilde{\xi}\tilde{\nu}\sqrt{2}\sqrt{1 - \frac{T_{11}^2}{K_{11}}}, \tag{42}$$

where $\tilde{\xi} \in \pm 1$. Equating (41) and (42) yields,

$$T_{21} = -\tilde{\xi}\sqrt{2} + \tilde{\nu}\frac{(K_{11} - \tilde{\mu}T_{11}^2)}{\sqrt{K_{11} - T_{11}^2}} \tag{43}$$

The key coefficient c in (36) is therefore

$$c = \sqrt{K_1}\left(\sqrt{K_1} - T_1\right) = \tilde{\xi}\tilde{\nu}\sqrt{2}\sqrt{K_{11} - T_{11}^2}, \tag{44}$$

and to ensure $c < 0$ (oscillations/AFM-like modulation), one must pick the $-$ branch for T_1 so that $T_1 > \sqrt{K_1}$. Furthermore, we need $\tilde{\xi}\tilde{\nu} = -1$.

The physical fields follow from $u = e^q$:

$$\begin{aligned} A &= -\tfrac{T_2}{\beta}(\ln u)' = -\tilde{\mu}\sqrt{K_{11}}q', \\ h &= \alpha A' = -\tilde{\nu}\tilde{\mu}\sqrt{K_{11} - T_{11}^2}q''. \end{aligned} \tag{45}$$

A constructive protocol is now evident: fix $K_{11} > 0$; choose T_{11} with $T_{11}^2 < K_{11}$ (which sets β and hence θ); select T_{21} via (43); the remaining entries can be tuned within Γ to control stability (in particular, to permit loss of convexity, consistent with AFM coexistence at $H = 0$).

We next evaluate the 1D form of the energy by substituting the 1D ansatz (21) into the functional (14). This substitution yields the following expression for the energy when $H = 0$.

$$E = \int \left[\frac{(1-u^2)^2}{2} + K_1 (u')^2 + 2T_1\, u' A u + A^2 u^2 + (\alpha A')^2 \right] \mathrm{d}x. \quad (46)$$

With $u = e^q$ and $A = -(T_2/\beta)q'$, we obtain

$$E = \int \frac{(1-e^{2q})^2}{2} + e^{2q}(q')^2 \left(K_1 - \frac{2T_1 T_2}{\beta} + \frac{T_2^2}{\beta^2} \right) + \alpha^2 \frac{T_2^2}{\beta^2} (q'')^2 \, \mathrm{d}x. \quad (47)$$

Invoking the compatibility relations ($T_2^2/\beta^2 = K_{11}$, $\alpha^2 = 1 - T_{11}^2/K_{11}$) and branch choices gives the compact form

$$E = \int \frac{(1-e^{2q})^2}{2} - 2\tilde{\mu} e^{2q} (q')^2 \left(K_{11} - \tilde{\xi}\tilde{\nu}\sqrt{2}\sqrt{K_{11} - T_{11}^2} \right) + (K_{11} - T_{11}^2)(q'')^2 \, \mathrm{d}x. \quad (48)$$

Since $c = \tilde{\nu}\tilde{\xi}\sqrt{2}\sqrt{K_{11} - T_{11}^2}$, we may rewrite

$$E = \int \left[\frac{(1-e^{2q})^2}{2} - 2\tilde{\mu}(K_{11} - c) e^{2q} (q')^2 + \frac{c^2}{2} (q'')^2 \right] \mathrm{d}x. \quad (49)$$

Using $cq'' = -(1 - e^{2q})$, we have $\frac{(cq'')^2}{2} = \frac{(1-e^{2q})^2}{2}$ and therefore

$$E = \int \left[(1-e^{2q})^2 - 2\tilde{\mu}(K_{11} - c) e^{2q} (q')^2 \right] \mathrm{d}x. \quad (50)$$

We consider the case of orthorhombic symmetry. In the principal coordinate system, both $\underline{\underline{K}}_m$ and $\underline{\underline{T}}_m$ are diagonal. Consequently, their representations in any arbitrary frame are obtained through rotation. This observation also implies that $\underline{\underline{T}}_m$ remains symmetric under rotation.[c]

We solve (37) using the initial conditions $q(0) = 0.1$ and $q'(0) = 0$. The material parameters are chosen as $(\underline{\underline{K}}_m)_{11} = 1.0$, $(\underline{\underline{K}}_m)_{12} = 0.0$, $(\underline{\underline{K}}_m)_{22} = 1.0$, $(\underline{\underline{T}}_m)_{11} = 0.6$, $(\underline{\underline{T}}_m)_{22} = 0.32$, and $(\underline{\underline{T}}_m)_{12} = (\underline{\underline{T}}_m)_{21}$, with the latter determined from (43). We further set $\tilde{\mu} = \tilde{\nu} = -\tilde{\xi} = 1$.

For these parameters, the average energy computed over the domain $[0, 100]$ is -0.0186736, corresponding to $c = -1.13137$. The energy being negative implies that the antiferromagnetic phase is more favorable compared to the bulk superconducting phase at zero external fields. The plot is presented in Fig. 3.

We can go further and add quartic stabilizer terms. If convexity is lost in Γ, then we propose a different minimizer,

$$GL_{A,G}[u, \theta, \underline{A}; \underline{H}] := \int_\Omega \frac{(1-u^2)^2}{2} + \nabla u \otimes \nabla u : \mathbb{K} \nabla u \otimes \nabla u + \nabla u \cdot \underline{\underline{K}}_m \nabla u + 2\underline{\underline{T}}_m \nabla u \cdot \underline{A}_0 u + u^2 \underline{A}_0 \cdot \underline{\underline{M}}_m \underline{A}_0 + \underline{A}_0 u \otimes \underline{A}_0 u : \mathbb{M} \underline{A}_0 u \otimes \underline{A}_0 u \, \mathrm{d}x + \int_{\mathbb{R}^3} |\mathrm{curl} \underline{A} - \underline{H}|^2 \, \mathrm{d}x, \quad (51)$$

where the fourth-order tensors $\mathbb{K}$ and $\mathbb{M}$ have been added to bound the energy functional from below. Substituting in the 1D ansatz from (21), we end up with the following energy functional

$$GL_{A,G}[u, \theta, \underline{A}; \underline{H}] := \int \frac{(1-u^2)^2}{2} + \gamma_1 (u')^4 + K_1 (u')^2 + 2T_1 u' A u + u^2 A^2 + \gamma_2 (Au)^4 + |\alpha A'|^2 \, \mathrm{d}x, \quad (52)$$

where $\gamma_1 = \underline{d} \otimes \underline{d} : \mathbb{K} \underline{d} \otimes \underline{d}$ and $\gamma_2 = \underline{e} \otimes \underline{e} : \mathbb{M} \underline{e} \otimes \underline{e}$. As mentioned previously, we have set $\underline{\underline{M}} = \underline{\underline{I}}$, and we have restricted our attention to $\underline{H} = 0$. The other constants are as defined earlier.

Since we are interested in the antiferromagnetic phase, we consider the following perturbation ansatz.

$$\begin{aligned} u(s) &= 1 + \epsilon u_1(s) = 1 + \epsilon \cos(qs) \\ A(s) &= \epsilon A_1(s) = \epsilon \delta \sin(qs), \end{aligned} \quad (53)$$

where $s = \underline{x} \cdot \underline{d}$, q represents the length scale of oscillations and δ represents the relative amplitude of the magnetic oscillations and ϵ is a small parameter. Substituting (53) into (52), and assuming ϵ small leads to just retaining the quadratic terms. Minimizing over δ and q gives us the result

$$q^{*2} = \frac{1}{\alpha^2} \left(\frac{T_1}{\sqrt{K_1}} - 1 \right), \quad \delta^* = -\frac{T_1 q^*}{1 + \alpha^2 q^{*2}} \quad (54)$$

where for q^* to be real we need $T_1 > \sqrt{K_1}$ which is exactly the loss of convexity condition for Γ (see (20)). The magnitude of ϵ is determined by minimizing over the quartic terms. We assume that the material constants γ_1 and γ_2 are such that ϵ is small. From experiments on Sr_2RuO_4(50), it was determined that the antiferromagnetic domains are roughly 50 μm in size. We may use this to make a crude estimate for $\underline{\underline{T}}_m$. From the expression of q^*, we determine the value of $\underline{\underline{T}}_m$, the time reversal symmetry breaking term, to be of the order of 77.64×10^{-33} Cm. See Section S7 in the Supplementary material.

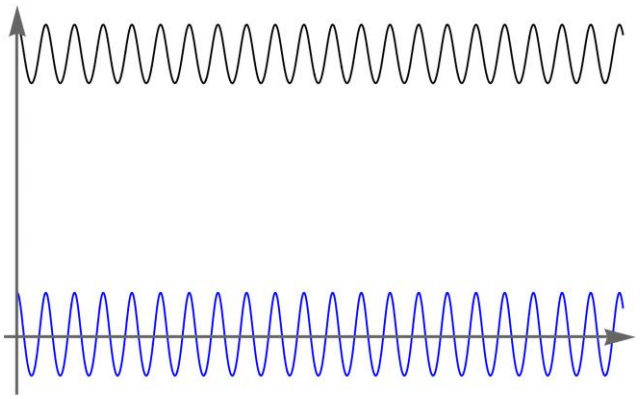

Figure 3 Plot of the antiferromagnetic instability phase. The order parameter is plotted in black, while the magnetic field is plotted in blue. Assuming orthorhombic symmetry, we chose $(\underline{\underline{K}}_m)_{11} = 1$, $(\underline{\underline{K}}_m)_{12} = 0.0$, $(\underline{\underline{K}}_m)_{22} = 1.0$, $(\underline{\underline{T}}_m)_{11} = 0.6$, $(\underline{\underline{T}}_m)_{22} = 0.32$, and $(\underline{\underline{T}}_m)_{12} = (\underline{\underline{T}}_m)_{21}$ determined via (43).

Consequences

Now, we explore the consequences of our results in relation to experimental observation. We consider two cases:

direction-dependent surface energy (case 1) and the coexistence of superconductivity and magnetism (case 2). Case 1 further divides into scenarios where surface energy becomes negative (case 1a) or remains positive but varies with direction (case 1b).

Case 1a: Negative surface energy

When the surface energy becomes negative along a given direction, the system can lower its overall energy by forming laminates oriented along that direction. These predicted laminates should be observable using the Bitter pattern method, in which ferromagnetic or diamagnetic particles, with sizes as small as 10 nm, are deposited on the material surface under an applied magnetic field (18, 51). The differential accumulation of particles distinguishes superconducting and normal domains (17, 18, 52). The resulting patterns are expected to resemble the Landau laminate structures seen in type I superconductors (28, 29). It is worth noting that when the surface energy becomes negative, the system energetically favors increasing interfacial area, which, in a purely continuum description, would suggest refinement of the laminate structure to arbitrarily small length scales. However, such refinement cannot proceed indefinitely in physical systems. The present framework is based on a continuum Ginzburg–Landau description, which is expected to break down at microscopic length scales. In particular, we expect the refinement to be arrested at a lower cutoff set by intrinsic material length scales, between the superconducting coherence length and microscopic electronic length scales associated with the underlying quantum structure (Fermi wave vector). A conservative estimate suggests that this lower bound lies in the range of ∼0.01 to 0.1 μm. The smallest particle size for Bitter pattern experiments are ∼0.01 μm (51), so length scales below this might not be distinguishable by bitter pattern experiments. Interestingly, the characteristic length scales observed in intermediate-state patterns are typically in the range of 0.1 to 1 μm. The overlap between these scales may provide a plausible explanation for why such effects have not been distinctly identified in prior experimental studies, as the refinement predicted by the present model would be difficult to resolve within the experimentally accessible regime. In light of this, we discuss the similarities and differences between the predicted behavior and experimental observations. The key similarities include:

1. **Laminate formation**: Both show alternating superconducting and normal domains in Bitter experiments.
2. **Branching near surfaces**: Similar to Landau laminates, case 1a should exhibit branching patterns due to magnetic field spreading (11, 18). Thus, experiments done on samples below a critical thickness should minimize branching observed at the surface (18).
3. **Volume fraction**: Coexistence of superconducting and normal phase leads to fixing the volume fraction of the phases (see "Microscopic structure of the intermediate state" in (28) or "2.3.2 Intermediate state in a flat slab" in (29)). We expect this to be the same for both case 1a and the Landau laminate solution.
4. **Polycrystalline behavior**: Polycrystalline samples exhibit isotropic behavior. As previously noted, the isotropic form of our modified functional maps to the isotropic Ginzburg–Landau functional via (11), and therefore cannot be used to distinguish between the two models.

The dissimilarities manifest for the single crystal case:

1. **Single crystals**: Unlike Landau laminates, where the pattern appears along different directions, case 1a favors a single direction dictated by the negative surface energy.
2. **Influence of field direction**: Since laminate orientation in the intermediate state is nucleation-dependent, an inclined magnetic field tends to align the laminates along its in-plane component (see Shavrin geometry (18, 20)). In contrast, case 1a possesses an intrinsic directional preference that, we predict, will remain unaffected by small in-plane components of the applied field.
3. **Competition with vortex phase**: It is instructive to compare the energetic contributions of case 1a and the vortex phase. Case 1a exhibits negative surface energy along a specific direction, whereas the vortex phase possesses negative surface energy along all directions. In the vortex phase, the surface energy is computed per unit area (planar problem), as vortices are localized flux tubes. In contrast, the surface energy for case 1a is per unit length, as the laminate phase extends uniformly in the direction of the domain wall. Thus for long enough samples, the total surface energy for case 1a will dominate that of the vortex phase. The surface energy grows with length in case 1a, but is independent of length for the vortex. Thus, there exists a critical length of the sample geometry for the stability of case 1a.

It is worth noting that even when $\underline{\underline{T}}_m \neq 0$, the surface energy continues to depend on the orientation of the domain wall. However, the presence of a nonzero $\underline{\underline{T}}_m$ introduces the possibility of nontrivial magnetic behavior within the resulting patterns. Consequently, the corresponding Bitter-pattern experiments are expected to display distinct signatures compared to conventional superconductors.

To clearly distinguish between superconducting and magnetic domains, one may complement Bitter-pattern imaging with magneto-optic Kerr effect measurements, thereby identifying regions that are superconducting versus those that exhibit diamagnetism.

Case 1b: Directional dependence of surface energy

In energy minimization, phase coexistence of domains imposes constraints on the volume fraction, but not on the orientation of the domains. The orientation of the domain is typically nucleation dependent. In case 1b, where the surface energy is positive, but direction dependent, we expect a preferred domain orientation. The equilibrium domain configuration follows Wulff's construction (47, 48), leading to polyhedral domains with elongated structures along low-energy directions. While the present framework predicts the existence and orientation of anisotropic domains, the precise magnitude of the anisotropy (eg aspect ratios) depends on material-specific parameters and is not uniquely determined within the current formulation. Nevertheless, the deviation from isotropic domain morphology and the emergence

of preferred orientations distinguish this case from classical isotropic Ginzburg–Landau behavior. MgB_2 exhibits such behavior, where domains show preferred orientations (53). We present our interpretation of Bitter pattern experiments in Ref. (53). See Section S6 in the Supplementary material for detailed discussion.

Case 2: Coexistence of superconductivity and magnetism

Unlike conventional Ginzburg–Landau theory, which prohibits superconductivity and magnetism from coexisting, case 2 predicts superconducting states with alternating magnetic domains (Figure 3). Experimentally, such behavior is seen in UTe_2, $ErNi_2B_2C$, Sr_2RuO_4, and ternary rare-earth superconductors (40–42, 50). These materials show two distinct transitions: normal to superconducting, and superconducting to antiferromagnetic superconducting. Sometimes the second transition merges with the first. The latter transition suggests an emergent phase, analogous to our modification (refer to the discussion in Loss of stability section above), inducing nontrivial superconducting states.

From Fig. 3, we observe alternating sign changes in $B = \mathcal{f} - \mathrm{curl}A = H + M$, indicating an antiferromagnetic superconducting phase since $H = 0$. This suggests $\underline{\underline{T}}_m = 0$ at higher temperatures, becoming nonzero at lower temperatures and breaking convexity of Γ in (20). Notably, experimental observations in systems such as Sr_2RuO_4 indicate that the characteristic length scale of these antiferromagnetic oscillations is on the order of 50 μm (50), which is consistent with the spatially modulated structures predicted by the present framework. Various experimental methods—including Kerr rotation, muon spin resonance, and nuclear magnetic resonance (NMR)—have confirmed such states, supporting the presence of antiferromagnetic states in real materials. Further, a lot of these materials show antiferromagnetic behavior at zero applied external field.

Conclusion

We have proposed a minimal yet fundamental modification to the Ginzburg–Landau framework that naturally predicts the coexistence of superconductivity and magnetism. The TRSB modification is suspected to be the source of these nontrivial predictions. Reformulated in gauge-invariant variables, the model introduces a coupling term consistent with all underlying symmetries, thereby revealing physical phenomena absent in the classical theory. In the isotropic limit, this modification results in no modification, whereas its anisotropic extension yields direction-dependent surface energies and oscillatory superconducting states reminiscent of antiferromagnetic order.

For case 1a, we have outlined clear experimental pathways for validation, since there is a possibility that these phases may have been misclassified as intermediate states in type-I superconductors. In case 1b, we identified a representative material system and demonstrated that the surface energy depends sensitively on the orientation of the domain wall. This directional dependence implies that certain domain wall orientations are energetically preferred, suggesting that experimental observations of anisotropic or faceted domain patterns could directly verify the theoretical predictions. We further showed that an antiferromagnetic ground state at zero external field is brought about by a loss of convexity in the tensor Γ (see Loss of stability section above). The theoretical framework and these key mechanisms are further supported by experimental evidence from the materials discussed in case 2, which exhibit both superconducting and magnetic order consistent with our predictions. It is worth emphasizing that several materials—such as MgB_2 and UTe_2—are currently modeled in the literature using multicomponent order parameters to capture such coexistence phenomena. Our analysis suggests that these behaviors may, in fact, arise from a richer thermodynamic functional even within a single-component order parameter framework. From a continuum thermodynamics standpoint, enriching the energy functional is a more natural and parsimonious extension of theory than increasing the number of state variables. This perspective offers a unified and conceptually economical route to modeling complex superconducting materials.

Notes

[a]It is often assumed that any energy functional describing superconductivity must be analytic with respect to the order parameter ψ, its gradient $\nabla\psi$, and their complex conjugates. The functional considered here does not satisfy this assumption. However, we view Ginzburg–Landau theory as a thermodynamic framework whose fundamental dependence should be on physically observable quantities—specifically, the magnitude $|\psi|$ and a gauge-invariant vector potential. Since the complex order parameter ψ itself is not directly observable, there is no fundamental requirement that the free energy be analytic in ψ. The present modification is fully gauge invariant and is formulated entirely in terms of observable fields, and is therefore well defined within this thermodynamic perspective.

[b]We have also normalized $u \mapsto u/\sqrt{\hat{\alpha}/\hat{\beta}}$ similar to the isotropic case in Reformulation of the Ginzburg–Landau model for the isotropic case section.

[c]$\underline{\underline{T}}_m$ need not be symmetric in general.

Acknowledgments

P.S. acknowledges support of NSF grant 2437028 and the Cullen Chair from the University of Houston. L.L. acknowledges NSF grant 2437029.

Supplementary material

Supplementary material is available at *PNAS Nexus* online.

Competing interest

The authors declare no competing interests.

Funding

This work is supported in part by funds from the National Science Foundation (NSF: # 2437028 and # 2437029).

Author contributions

P.S. and L.L. conceived the concept, S.S. conducted the theoretical derivations and computations, and all authors analyzed the

results. S.S. wrote the initial draft, and all authors edited and reviewed the manuscript.

Data availability

All data are included in the manuscript and the Supplementary information document.

References

1. Ginzburg L, Landau LD. 1950. On the theory of superconductivity. *Zhurnal Eksperimental'noi i Teoreticheskoi Fiziki*. 20: 1064–1082.
2. Ter Haar D. *Collected papers of LD Landau*. Elsevier, 2013.
3. Meissner W, Ochsenfeld R. 1933. Ein neuer effekt bei eintritt der supraleitfähigkeit. *Naturwissenschaften*. 21:787–788.
4. Gorter CJ, Casimir H. 1934. On supraconductivity I. *Physica*. 1: 306–320.
5. Langevin P. 1911. Rapp. et disc. du ler conseil solvay.
6. Keesom WH, Kok JA. 1934. Measurements of the specific heat of thallium at liquid helium temperatures. *Physica*. 1:175–181.
7. Kok JA. 1934. Some remarks on supraconductivity and fermi-dirac statistics. *Physica*. 1:1103–1106.
8. Keesom WH, Ende JvdComm. leiden.
9. Peierls R. 1936. Magnetic transition curves of supraconductors. *Proc R Soc Lond A Math Phys Sci*. 155:613–628.
10. Ginzburg VL, Landau LD. *On the theory of superconductivity*. Springer, 2009.
11. Landau L. 1938. The intermediate state of supraconductors. *Nature*. 141:688–688.
12. Landau LD. 1943. On the theory of the intermediate state of superconductors. *J Phys USSR*. 7:99.
13. Lifshitz EM, Sharvin YV, Sykes JB. *The intermediate state of superconductors*. In: *Perspectives in theoretical physics*. Elsevier; 1992. p. 299–302.
14. Faber TE. 1958. The intermediate state in superconducting plates. *Proc R Soc Lond A Math Phys Sci*. 248:460–481.
15. Choksi R, Kohn RV, Otto F. 2004. Energy minimization and flux domain structure in the intermediate state of a type-i superconductor. *J Nonlinear Sci*. 14:119–171.
16. Conti S, Otto F, Serfaty S. 2016. Branched microstructures in the Ginzburg–Landau model of type-I superconductors. *SIAM J Math Anal*. 48:2994–3034.
17. DeSorbo W, Healy WA. 1964. The intermediate state of some superconductors. *Cryogenics (Guildf)*. 4:257–323.
18. Huebener RP. *Magnetic flux structures in superconductors: extended reprint of a classic text*. Vol. 6. Springer Science & Business Media, 2013.
19. Haenssler F, Rinderer L. 1965. Topologie de la structure de letat intermediaire des supraconducteurs du type i et mesure de lenergie de surface. *Helv Phys ACTA*. 38:448.
20. Sharvin YV, Landau IL. 1970. Investigation of the dynamic intermediate state of superconductors. *Sov Phys JETP*. 31: 1047–1053.
21. Bodmer A, Essmann U, Träuble H. 1972. The intermediate state in thin lead and tin specimens. *Phys Status Solidi A Appl Mater Sci*. 13:471–481.
22. Abrikosov AA. 1957. On the magnetic properties of superconductors of the second group. *Sov Phys-JETP*. 5:1174–1182.
23. Essmann U, Träuble H. 1967. The direct observation of individual flux lines in type ii superconductors. *Phys Lett A*. 24: 526–527.
24. Wells FS, Pan AV, Wang XR, Fedoseev SA, Hilgenkamp H. 2015. Analysis of low-field isotropic vortex glass containing vortex groups in yba2cu3o7- x thin films visualized by scanning squid microscopy. *Sci Rep*. 5:8677.
25. Kleiner WH, Roth LM, Autler SH. 1964. Bulk solution of ginzburg-landau equations for type ii superconductors: upper critical field region. *Phys Rev*. 133:A1226–A1227.
26. Brandt EH. 1972. Ginsburg-landau theory of the vortex lattice in type-ii superconductors for all values of x and b. *Phys Status Solidi B Basic Solid State Phys*. 51:345–358.
27. Saint-James D, Sarma G, John Thomas E. 1969. Type-II superconductivity. Technical Report, CEN, Saclay, France.
28. Gennes P-GD. *Superconductivity of metals and alloys*. CRC Press, 2018.
29. Tinkham M. *Introduction to superconductivity*. Courier Corporation, 2004.
30. Saint-James D, de Gennes PG. 1963. Onset of superconductivity in decreasing fields. *Phys Lett A*. 7:306–308.
31. Almog Y. 1999. Asymptotic analysis of the one-dimensional Ginzburg-Landau equations near self-duality. *Q Appl Math*. 57:355–367.
32. Matricon J, Saint-James D. 1967. Superheating fields in superconductors. *Phys Lett A*. 24:241–242.
33. Jon Chapman S. 1994. Nucleation of superconductivity in decreasing fields. I. *Eur J Appl Math*. 5:449–468.
34. Chapman SJ. 1995. Asymptotic analysis of the ginzburg-landau model of superconductivity: reduction to a free boundary model. *Q Appl Math*. 53:601–627.
35. Chapman S, Du Q, Gunzburger M, Peterson J. 1995. Simplified ginzburg-landau models for superconductivity valid for high kappa and high fields. *Adv Math Sci Appl*. 5: 193–218.
36. Wysokiński KI. 2019. Time reversal symmetry breaking superconductors: Sr2RuO4 and beyond. *Condens Matter*. 4:47.
37. Robins A, Brydon P. 2018. Time-reversal symmetry-breaking in noncentrosymmetric superconductors. *J Phys Condens Matter*. 30:405602.
38. Poniatowski NR, Curtis JB, Yacoby A, Narang P. 2022. Spectroscopic signatures of time-reversal symmetry breaking superconductivity. *Commun Phys*. 5:44.
39. Gurtin ME. 1995. Dynamical theories of electromagnetism and superconductivity based on gauge invariance and energy.
40. Maple MB, Fischer Ø. *Magnetic superconductors*. In: *Superconductivity in ternary compounds ii: superconductivity and magnetism*. Springer; 1982. p. 1–10.
41. Yaron U, *et al.* 1996. Microscopic coexistence of magnetism and superconductivity in ErNi2B2C. *Nature*. 382:236–238.
42. Hayes IM, *et al.* 2021. Multicomponent superconducting order parameter in UTe2. *Science*. 373:797–801.
43. Kapitulnik A, Xia J, Schemm E, Palevski A. 2009. Polar Kerr effect as probe for time-reversal symmetry breaking in unconventional superconductors. *New J Phys*. 11:055060.
44. Levenson-Falk EM, Schemm ER, Aoki Y, Maple MB, Kapitulnik A. 2018. Polar Kerr effect from time-reversal symmetry breaking in the heavy-fermion superconductor pros 4 sb 12. *Phys Rev Lett*. 120:187004.

45. Wei DS, *et al.* 2022. Interplay between magnetism and superconductivity in UTe 2. *Phys Rev B*. 105:024521.
46. Bernhard C, *et al.* 1999. Coexistence of ferromagnetism and superconductivity in the hybrid ruthenate-cuprate compound RuSr 2 GdCu 2 O 8 studied by muon spin rotation and DC magnetization. *Phys Rev B*. 59:14099–14107.
47. Herring C. 1951. Some theorems on the free energies of crystal surfaces. *Phys Rev*. 82:87–93.
48. Liu WB, *et al.* 2016. Effects of surface energy anisotropy on void evolution during irradiation: a phase-field model. *J Nucl Mater*. 479:316–322.
49. Klemm RA, Clem JR. 1980. Lower critical field of an anisotropic type-II superconductor. *Phys Rev B*. 21:1868.
50. Xia J, Maeno Y, Beyersdorf PT, Fejer MM, Kapitulnik A. 2006. High resolution polar Kerr effect measurements of Sr 2 RuO 4: evidence for broken time-reversal symmetry in the superconducting state. *Phys Rev Lett*. 97:167002.
51. Kitakami O, Sakurai T, Shimada Y. 1996. High density recorded patterns observed by high-resolution bitter scanning electron microscope method. *J Appl Phys*. 79: 6074–6076.
52. Haenssler F, Rinderer L. 1967. Statistics and dynamics of the intermediate state of superconductors of type i. Technical report, Univ., Lausanne, Switzerland.
53. Moshchalkov V, *et al.* 2009. Type-1.5 superconductivity. *Phys Rev Lett*. 102:117001.